EBioMedicine 33 (2018) 196–210

Contents lists available at ScienceDirect

EBioMedicine

journal homepage: www.ebiomedicine.com

Research Paper

IL-33 Initiates Vascular Remodelling in Hypoxic Pulmonary Hypertension by up-Regulating HIF-1α and VEGF Expression in Vascular Endothelial Cells

Jie Liu [a,b], Wang Wang [b], Lei Wang [b], Shihao Chen [a], Bo Tian [c], Kewu Huang [d], Chris J. Corrigan [e], Sun Ying [a], Wei Wang [a,*], Chen Wang [f]

[a] The Department of Immunology, School of Basic Medical Sciences, Capital Medical University, Beijing, China
[b] The Department of Physiology and Pathological Physiology, School of Basic Medical Sciences, Capital Medical University, Beijing, China
[c] Department of Thoracic Surgery, Beijing Chao-Yang Hospital, Capital Medical University & Beijing Institute of Respiratory Medicine, Beijing, China
[d] Department of Respiratory and Critical Care Medicine, Beijing Chao-Yang Hospital, Capital Medical University & Beijing Institute of Respiratory Medicine, Beijing, China
[e] Faculty of Life Sciences & Medicine, School of Immunology & Microbial Sciences, Department of Inflammation Biology, Asthma UK Centre in Allergic Mechanisms of Asthma, King's College London, London, UK
[f] The Department of Respirology, Capital Medical University, Beijing, China

ARTICLE INFO

Article history:
Received 11 May 2018
Received in revised form 3 June 2018
Accepted 6 June 2018
Available online 18 June 2018

Keywords:
IL-33
Hypoxic pulmonary hypertension
Hypoxia inducible factor 1
Vascular endothelial growth factor

ABSTRACT

IL-33 may play a role in the vascular remodelling of hypoxic pulmonary hypertension (PH) but the precise mechanisms are still unclear. We hypothesized that hypoxia promotes expression of IL-33 and its receptor ST2 on vascular endothelial cells, which in turn leads to dysfunction of vascular endothelial cells and smooth muscle cells contributing to PH. Immunohistochemistry showed that immunoreactivity for IL-33 and ST2 was significantly increased in lung tissue of murine model of hypoxia-induced PH (HPH) and of subjects with bronchiectasis-PH. *trans*-Thoracic echocardiography showed that haemodynamic changes and right ventricular hypertrophy associated with HPH were significantly abrogated in $St2^{-/-}$ compared with WT mice. Administration of IL-33 further exacerbated these changes in the hypoxia-exposed WT mice. *In vitro*, hypoxia significantly increased IL-33/ST2 expression by human pulmonary arterial endothelial cells (HPAECs), while exogenous IL-33 enhanced proliferation, adhesiveness and spontaneous angiogenesis of HPAECs. Knockdown of endogenous *Il33* or *St2* using siRNA transfection significantly suppressed these effects in both normoxic and hypoxic culture-conditions. Deletion of the *St2* gene attenuated hypoxia-induced, elevated lung expression of HIF-1α/VEGFA/VEGFR-2/ICAM-1, while administration of exogenous VEGFA partially reversed the attenuation of the haemodynamic indices of PH. Correspondingly, knockdown of the *St2* or *Hif1α* genes almost completely abrogated IL-33-induced expression of HIF-1α/VEGFA/VEGFR-2 by HPAECs *in vitro*. Further, IL-33-induced angiogenesis by HPAECs was extensively abrogated by knockdown of the *Hif1α*/*Vegfa* or *Vegfr2* genes. These data suggest that hypoxia induces elevated expression of IL-33/ST2 by HPAECs which, at least partly by increasing downstream expression of HIF-1α and VEGF initiates vascular remodelling resulting in HPH.

1. Introduction

Hypoxic pulmonary hypertension (HPH) is commonly observed in the context of chronic hypoxia caused by a variety of lung diseases [1, 2]. Although the precise mechanisms of HPH are largely unknown, hypoxia enhanced pulmonary vasoconstriction and vascular remodelling are considered to be the two major pathogenic processes of HPH, resulting in elevated pulmonary vascular resistance and consequent pulmonary artery pressure with eventual cardiac hypertrophy and failure. The process of vascular remodelling involves many factors including local inflammation, dysfunction and abnormal proliferation of vascular endothelial cells, smooth muscle cells and fibroblasts, although hypoxia is regarded as the key driver [3, 4].

IL-33, a member of the IL-1 family of cytokines expressed most prominently at epithelial and endothelial surfaces, acts by binding to the membrane receptors ST2 and IL-1RAcP (IL-1 receptor accessory protein), in a number of lung diseases involving pulmonary and pulmonary vascular remodelling [5–9]. It is therefore reasonable to hypothesize that IL-33 also contributes to the vascular remodelling processes of HPH through actions on vascular

* Corresponding author at: The Department of Immunology, School of Basic Medical Sciences, Capital Medical University, 10# Xi Tou Tiao, You An Men Wai, Fengtai District, Beijing 100069, China.
E-mail address: wy_robin@ccmu.edu.cn (W. Wang).

https://doi.org/10.1016/j.ebiom.2018.06.003

Research in context

Evidence before this study

We have been focusing on the role of cytokines in the pathogenesis of chronic pulmonary diseases for a long time, including asthma, COPD, fibrosis and bronchiectasis. We and others found that IL-33 might contribute to the occurrence and prognosis of many other diseases through binding its receptor ST2. Based on these findings, we were very eager to know whether IL-33/ST2 axis also exerts a role in hypoxia-induced pulmonary hypertension (HPH), a complication of many chronic respiratory diseases. Although it is well known that HIF-1α and VEGF play critical role in this complication, it is still unclear what the upstream of HIF-1α and VEGF is. Therefore, we first tested immunoreactivity for IL-33 and its receptor ST2 in the lung tissue sections derived from surgical specimens and from our established murine models of HPH. Surprisingly, we noted the increased immunoreactivity for both targets in these tissue sections. These findings inspired us to further explore the details of IL-33/ST2 in the pathogenesis of HPH.

Added Value of This Study

HPH is a life-threatening complication because there is lack of effective treatment. Although pulmonary arteries and ventricular remodeling might be mainly involved in the pathogenesis of the disease, the precise mechanisms are largely unknown. In the present study, we showed that hypoxia is a critical driver which induced expression of IL-33 and ST2 by endothelial cells. These factors, in turn triggered expression of HIF-1α and VEGF by endothelial cells and led to proliferation, adhesion and tube formation of these cells. We also showed that in the presence of IL-33, endothelial cells were able to affect proliferation and migration of artery smooth muscle cells, although IL-33 alone did not have such effects. These findings suggest that hypoxia and IL-33/ST2 might be initiators for HPH, through regulating downstream factors HIF-1α and VEGF.

Implications of all the Available Evidence

Our data suggest that IL-33/ST2 axis plays critical role in the pathogenesis of hypoxia-induced pulmonary hypertension because depletion of these molecules much remitted the phenomenon of complication. These observations might provide alternative therapeutic strategy for clinical treatment of HPH.

endothelial cells. In addition, vascular endothelial cell growth factor (VEGF) is a key "end effector" molecule in the vascular remodelling of HPH, which promotes angiogenesis by regulating the proliferation, migration and differentiation of endothelial cells [1–3]. The expression of VEGF is in turn regulated by the "molecular switch" molecule hypoxia-induced factor 1-alpha (HIF-1α) [10, 11]. A recent study has reported that HIF-1α may interact with the IL-33 promoter region, resulting in induction by HIF-1α of IL-33 expression in intestinal epithelial cells [12]. Other studies have shown that IL-33 promotes VEGF production by skin mast cells and the human keratinocyte cell line HaCaT [13, 14]. However, possible interactions between the IL-33/ST2 and HIF-1α/VEGF axes in the pathogenesis of HPH have not so far been addressed. We, here aimed to explore the role of both axes in the pathogenesis of the hypoxic pulmonary vascular remodelling which results in HPH.

2. Methods

2.1. Pulmonary Surgical Specimens

Collection of human lung tissues was approved by the Research Ethics Committee of Beijing Chao-yang Hospital. Prior written, informed consent was obtained from all patients to donate lung tissues. Surgical specimens of lung tissue were collected from patients with bronchiectasis-induced pulmonary hypertension (PH) ($n = 3$) and normal donor lungs removed following accidental death for 3 patients undergoing lung transplantation in the Beijing Chao-Yang Hospital, Capital Medical University, Beijing, China. Lung tissues were fixed in 10% formaldehyde then embedded in paraffin.

2.2. Animal Models

Male C57BL/6 and BALB/c mice (8 weeks) were purchased from the Vital River Laboratory Animal Technology Company of Beijing in China. $St2^{-/-}$ mice (BALB/c background) were a kind gift from Professor Andrew N.J. McKenzie of the Medical Research Council Laboratory of Molecular Biology, Cambridge, United Kingdom [15]. All experiments were undertaken with approval of the Institutional Animal Care and Use Committee (IACUC). Mice were randomly divided into two groups which were exposed to normal air or mixed air containing 10% oxygen in a normobaric chamber (BioSpherix, USA) for 4 weeks. The chamber was partially ventilated and equipped with an external oxygen controller which sensed the ambient oxygen concentration and replaced it with nitrogen when necessary. Cages were opened for cleaning every 3 days for 30 min.

2.3. Measurements of Haemodynamics in the Murine Model of HPH

The measurements were performed as previously described [16, 17]. Following anaesthesia of the mice with 2% sodium pentobarbital (50 mg/kg i.p.), right ventricular systolic pressure (RVSP), conventionally used as an indicator of mean pulmonary arterial pressure, was measured by closed-chest puncture of the right ventricle (RV) with a transducer attached to the PowerLab system (ADInstruments, Australia) as previously described [16]. A blood sample was then taken by cardiac apex puncture for haematocrit analysis (Radiometer, Denmark). Serum was stored in aliquots at −80 °C. Following euthanisation, the murine lungs and hearts were collected and the weights of the right ventricles (RV) and left ventricles including the interventricular septa (LV + S) measured separately to evaluate the right ventricular hypertrophy index (RVHI), which reflects right ventricular remodelling, as calculated by the formula: RVHI (%) = RV/(LV + S) × 100. The ratio of RV weight to body weight was calculated as RV/Body weight [16]. The diameters of individual cardiomyocytes in histological sections of the left and right ventricular walls were measured as previously described [17].

2.4. Analysis of Lung Morphometrics in the Murine Model of HPH

The left lungs of the mice were embedded in paraffin, serially sectioned at a thickness of 4 μm then stained using haematoxylin and eosin (H&E) and immunostaining. With the aid of the H&E stain, all pulmonary vessels with external diameters <100 μm in entire left lung were selected and the medial thickness of these vessels quantified by immunofluorescent labelling with anti-α-SMA (1:200 dilution, Sigma-Aldrich, USA), visualised with second layer Fluor (AF) 488-labelled goat anti-mouse IgG (ZsBio, China). Medial thickness was calculated as a percentage of the external diameter of the vessels as follows: percentage medial thickness (%MT) = (external diameter − internal diameter)/external diameter × 100 [17]. The data were segregated into four groups based on the external

diameters of the vessels: 0–25, 26–50, 51–75 and 76–100 μm. Images of pulmonary vessels were captured with a Nikon microscope digital camera system and circumferences measured using its image analysis software as previously described [17].

2.5. Immunohistochemical Analysis

Immunoreactivity for IL-33 and ST2 was measured using a rabbit anti-IL-33 monoclonal antibody (1/200, Santa Cruz, CA) or rabbit anti-ST2 monoclonal antibody (1/200, Abcam, UK) and analyzed as described previously [16].

2.6. Cell Culture and Proliferation Assay

Human pulmonary arterial endothelial cells (HPAECs) and human pulmonary arterial smooth muscle cells (HPASMCs) (ScienCell Research Laboratories, USA) were cultured according to the instruction of the manufactures. Human pulmonary arterial endothelial cells (HPAECs) (3–6 passages, ScienCell Research Laboratories, USA) were cultured in complete Endothelial Cell Medium (ECM). Cells were maintained in a CO_2 incubator (5%, Thermo, USA) at 37 °C and used for experiments at 80%–90% confluence. After starvation by culture in ECM containing 2% foetal bovine serum (FBS) to arrest growth for 4–6 h, cells were pretreated with either human recombinant IL-33 (rhIL-33) (10 ng/mL,

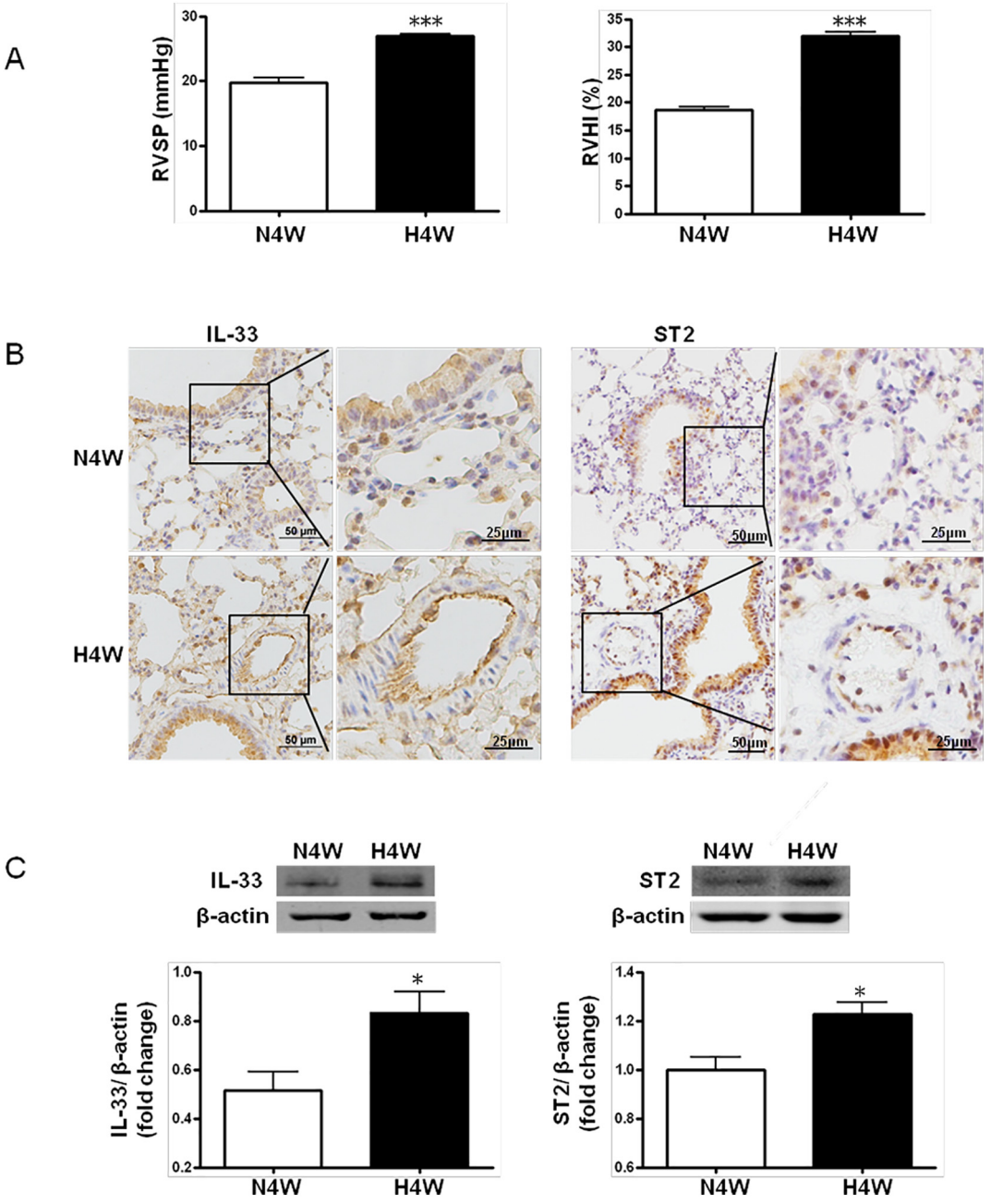

Fig. 1. Increased right ventricular systolic pressure (RVSP) and right ventricular hypertrophy index (RVHI) and elevated expression of IL-33 and ST2 immunoreactivity in lung sections from wild type mice exposed to normoxia(N4W)or to hypoxia (H4W) for 4 weeks. (A) RVSP and RVHI in murine models of hypoxia-induced murine PH (H4W) compared with control mice (N4W) ($n = 6$ each group). Data are presented as the mean ± SEM. ***$p < 0.001$. (B) Immunoreactivity for IL-33 and ST2 (brown) in murine lung tissue sections. (C) Western blot analysis of IL-33 and ST2 proteins (fold changes compared with β-actin) in lung tissue of murine models ($n = 4$–6 in each group). *$p < 0.05$.

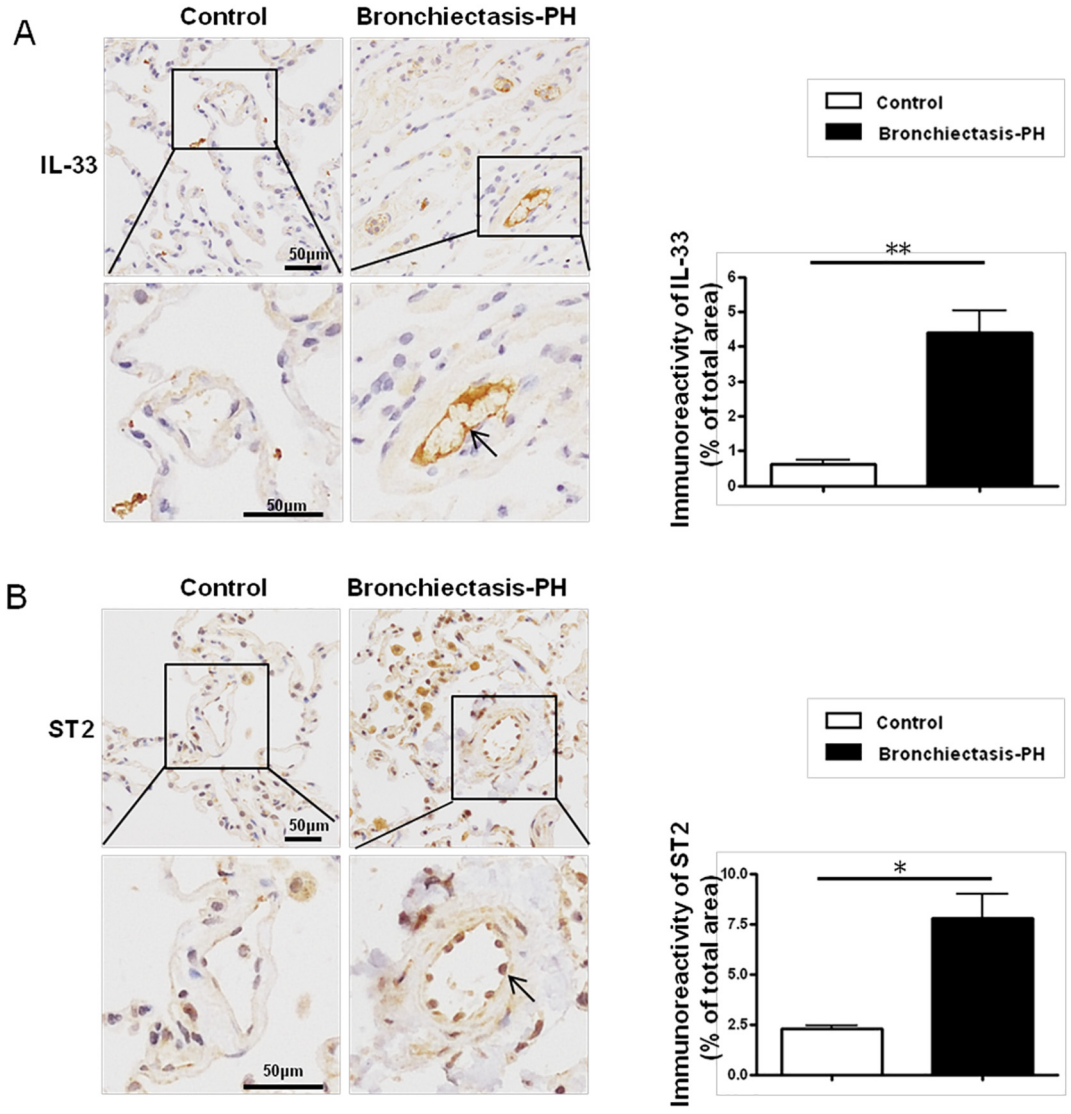

Fig. 2. Elevated expression of IL-33 and ST2 in patients with PH. (A and B) Immunoreactivity for IL-33 and ST2 (brown) in lung tissues from patients with bronchiectasis with PH and normal controls ($n = 3$ for each group). The arrows show pulmonary artery endothelia cells which are immunoreactive for IL-33 and ST2. Data are presented as the mean ± SEM. $^{**}p < 0.01$; $^{*}p < 0.05$.

R&D systems, MN, USA) or vehicle (PBS) in 5% FBS-ECM, followed by stimulation under conditions of hypoxia (3% oxygen) or normoxia (21% oxygen) for a further 24 h. Human pulmonary arterial smooth muscle cells (HPASMCs) (4–8 passages, ScienCell Research Laboratories) were cultured in complete smooth muscle cell medium (SMCM). Cells were maintained in a CO_2 incubator (5%, Thermo, USA) at 37°C and used for experiments at 80%–90% confluence.

Proliferation of HPAECs was assayed using a bromodeoxyuridine (BrdU) flow kit purchased from BD Pharmingen (BD Pharmingen, USA) according to the manufacturer's instructions. Briefly, HPAECs were seeded at 5×10^5cells per culture bottle and cultured for 24 h under different conditions. For analysis of DNA synthesis, cells were incubated with BrdU (10 μM) at 37 °C for 1 h. After collection, cells were treated with cytopermeabilisation/fixation medium (BD) then exposed to DNase (300 μg/mL dissolved in Dulbecco's Phosphate Buffered Saline, D-PBS) at 37 °C for a further 1 h. The incorporated BrdU was stained with specific anti-BrdU fluorescent antibody at room temperature for 20 min. A dye (7-aminoactinomycin D, 20 μL per sample) was added for staining of total DNA. Cells were analyzed using an LSRFortessa flow cytometer (Becton Dickinson, USA) which discriminated cells in S phase (P4), G0/G1 phase (P3), G2 phase (P5) and cells undergoing apoptosis (P6). The percentage of cells in S phase was calculated as P4/(P3 + P4 + P5) × 100%.

Proliferation of human pulmonary artery smooth muscle cells (HPASMCs) was measured using a commercial kit (Cell Counting Kit-

Fig. 3. Deletion of the *St2* gene reversed hypoxia-induced PH while IL-33 aggravated hypoxic pulmonary vascular remodelling. (A) Comparison of pulmonary vascular remodelling in wild type and $St2^{-/-}$ mice under conditions of normoxia and hypoxia: (top left panel) H&E staining of pulmonary arterioles; (bottom left panel) Immunofluorescent staining of α-SMA showing pulmonary arterioles; (right) Percentage medial thicknesses (%MT) of pulmonary arterioles categorised by external diameter into four groups (0–25 μm, 26–50 μm, 51–75 μm and 76–100 μm). $^{***}p < 0.001$ (*vs* N4W-WT: WT mice exposed to normoxia for 4 weeks); $^{\#\#\#}p < 0.001$ (*vs* H4W-WT: WT mice exposed to hypoxia for 4 weeks) (mean ± SEM of all arterioles in the entire left lung sections, $n = 6$ mice in each category). (B) Sections of cardiomyocytes from wild type and $St2^{-/-}$ mice exposed to normoxia and hypoxia. Cardiomyocyte hypertrophy was evident in the right ventricle (left panel), but not the left ventricle (right panel). $^{***}p < 0.001$ (*vs* WT mice under normoxia), $^{\#\#\#}p < 0.001$ (*vs* WT mice under hypoxia) (data show mean ± SEM of the diameter of 200 cardiomyocytes per section, $n = 6$ mice in each category). (C) RVSP, RVHI and RV/body weight ratio of wild type and $St2^{-/-}$ mice exposed to normoxia compared to hypoxia. $^{***}p < 0.001$ (*vs* wild type mice under normoxia), $^{\#\#\#}p < 0.001$ (*vs* wild type mice under hypoxia) (mean ± SEM, $n =$ 6–10 each group). (D) Administration of IL-33 aggravated hypoxic pulmonary vascular remodelling. (left panel) RVSP and RVHI of wild type mice exposed to hypoxia with or without IL-33. (middle panel) H&E staining of pulmonary arterioles from mice under hypoxia with or without exogenous IL-33. (right panel) %MT of pulmonary arterioles of mice exposed to hypoxia with or without exogenous IL-33 grouped by external diameter (mean ± SEM of all arterioles in the entire left lung sections, $n = 6$ mice in each group). $^{***}p < 0.001$, $^{**}p < 0.01$.

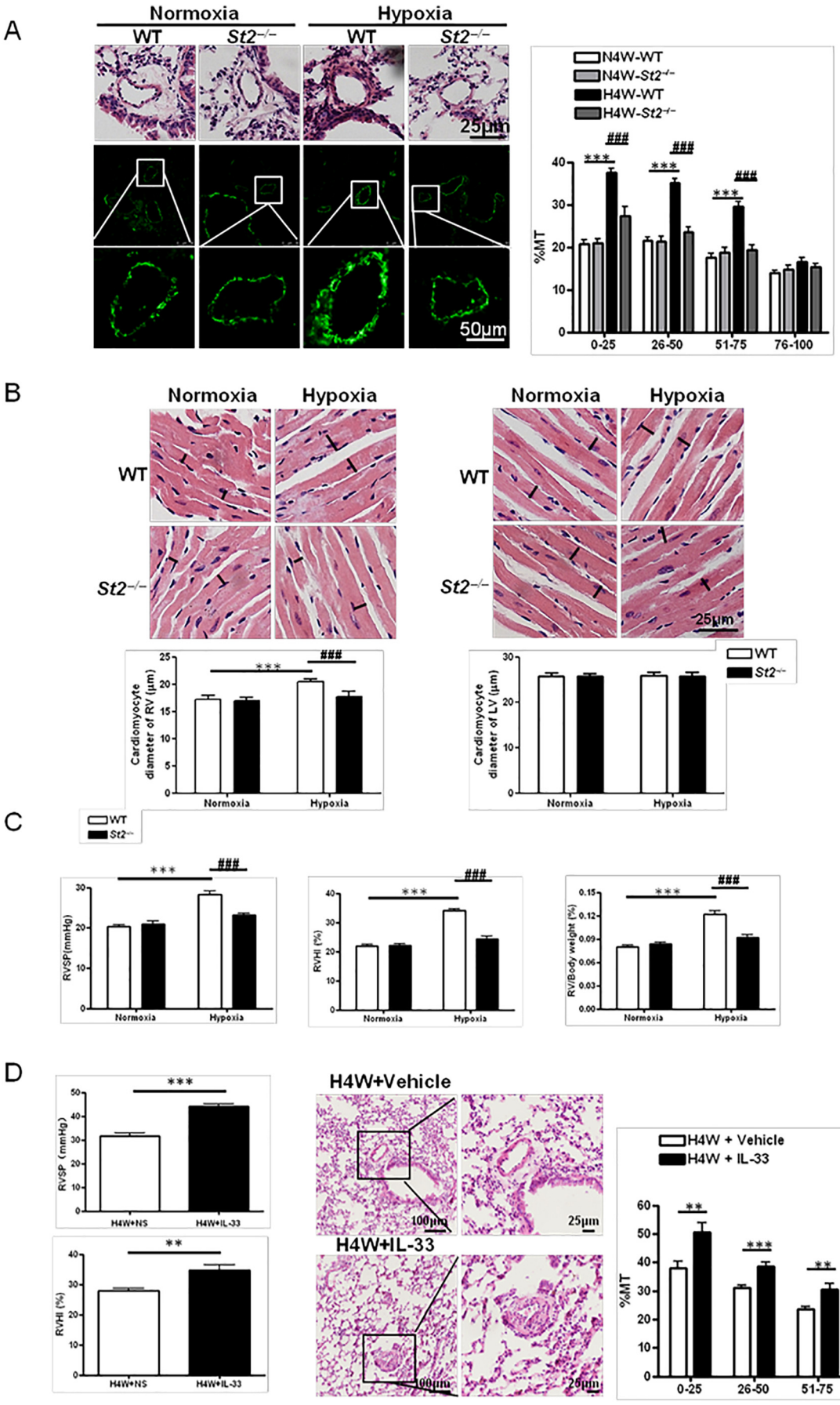
A
Normoxia
Hypoxia
WT
St2−/−
25μm
50μm
N4W-WT
N4W-St2−/−
H4W-WT
H4W-St2−/−
%MT
0-25
26-50
51-75
76-100
B
Cardiomyocyte diameter of RV (μm)
Cardiomyocyte diameter of LV (μm)
C
RVSP(mmHg)
RVHI (%)
RV/Body weight (%)
D
RVSP (mmHg)
H4W+NS
H4W+IL-33
H4W+Vehicle
H4W + Vehicle
H4W + IL-33

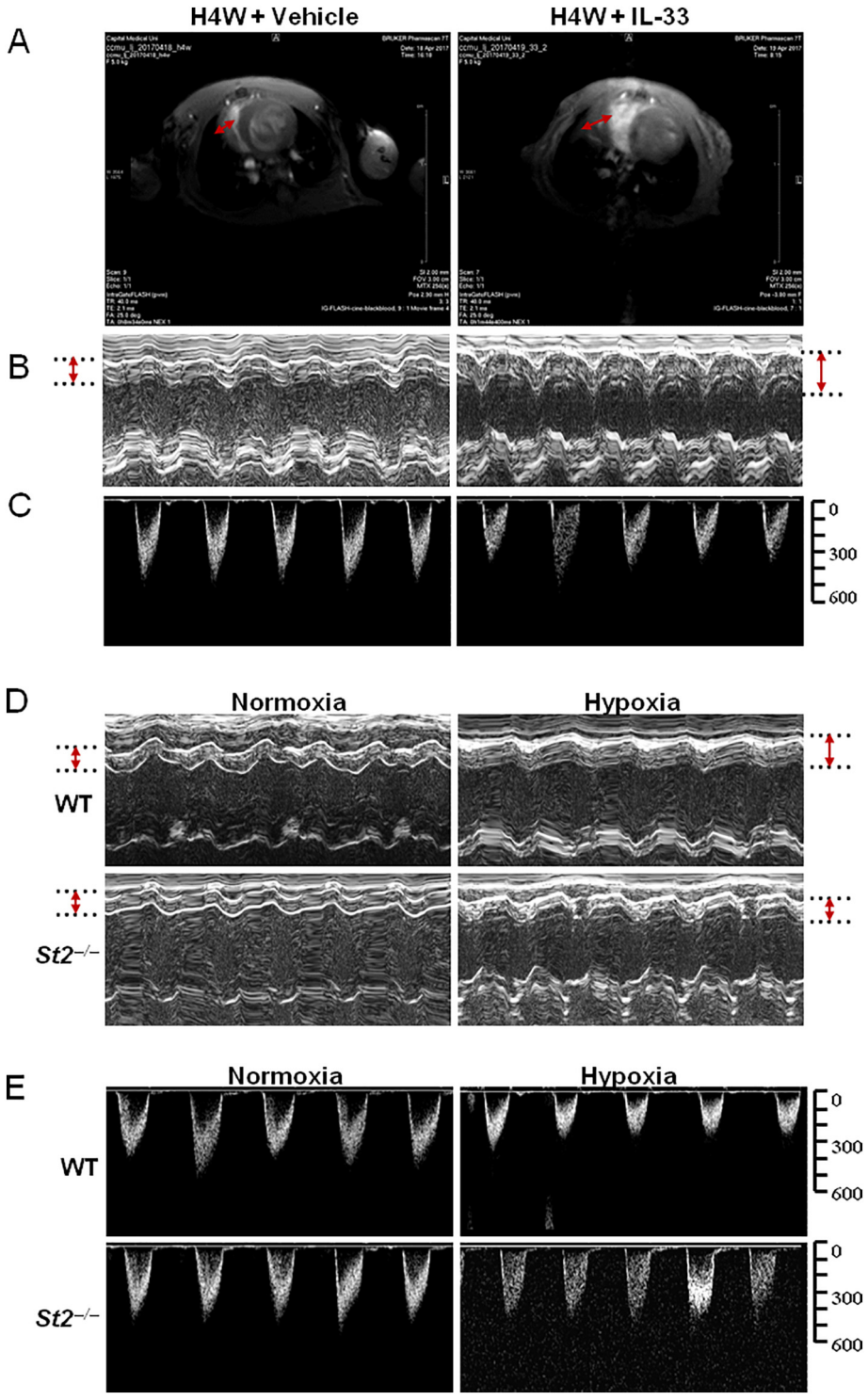

Fig. 4. Effects of exogenous IL-33 or of depletion of ST2 on RV wall thickness and the peak velocity of blood flow. IL-33 aggravates hypoxic pulmonary vascular remodelling. Magnetic resonance imaging (MRI) and M-mode trans-thoracic echocardiography showing typical cross sectional images of the heart (A), the thickness of the RV wall (B) and the PA peak flow velocity (C) in mice exposed to normobaric hypoxia concomitantly with exogenous IL-33 or normal saline for 4 weeks. Typical images showing changes of thickness of the RV wall (D, as indicated by arrow) and PA peak velocity (E) in WT and $St2^{-/-}$ mice exposed to normoxia or hypoxia. The results were measured by M-mode trans-thoracic echocardiography.

Fig. 5. Effects of exposure to hypoxia on expression of IL-33 by human pulmonary arterial endothelial cells (HPAECs) and effects of exogenous IL-33 on HPAECs. (A) Hypoxia-induced expression of IL-33 mRNA (left) and protein (right) by HPAECs ($n = 4$). $^{*}p < 0.05$, $^{**}p < 0.01$. (B) Effects of IL-33 on the cell cycle positions and DNA synthetic activities of HPAECs determined by analysing total DNA and incorporated BrdU using flow cytometry. The cells were treated with or without IL-33 for 24 h under normoxia. Gate P3 represents cells in G0/G1 phase, P4 is S phase, P5 is G2 + M phase, and P6 is apoptotic cells. $^{*}p < 0.05$, $n = 3$. (C) (left panel) Adhesion of HPAECs to culture plate wells in the presence of various concentrations of IL-33 under conditions of normoxia or hypoxia. Adherent cells were counted and expressed as the numbers of cells per high power field (5 wells for each group, and 6 HPFs in each well were counted). $^{***}p < 0.001$, $^{\#\#\#}p < 0.001$. (right panel) Adhesion of HPAECs following IL-33 gene knock down by siRNA under conditions of normoxia or hypoxia ($n = 5$). $^{**}p < 0.01$, $^{***}p < 0.001$. (D) (left panel) Spontaneous formation of capillaries (angiogenesis) by HPAECs cultured with IL-33 at various concentrations under conditions of normoxia or hypoxia. (right panel) Angiogenesis by HPAECs following IL-33 knock down by siRNA under conditions of normoxia or hypoxia. The results are expressed as the mean total tube lengths (percentages of medium control values) and numbers of tubes per field, respectively ($n = 6$). $^{**}p < 0.01$, $^{***}p < 0.001$, $^{\#\#\#}p < 0.001$.

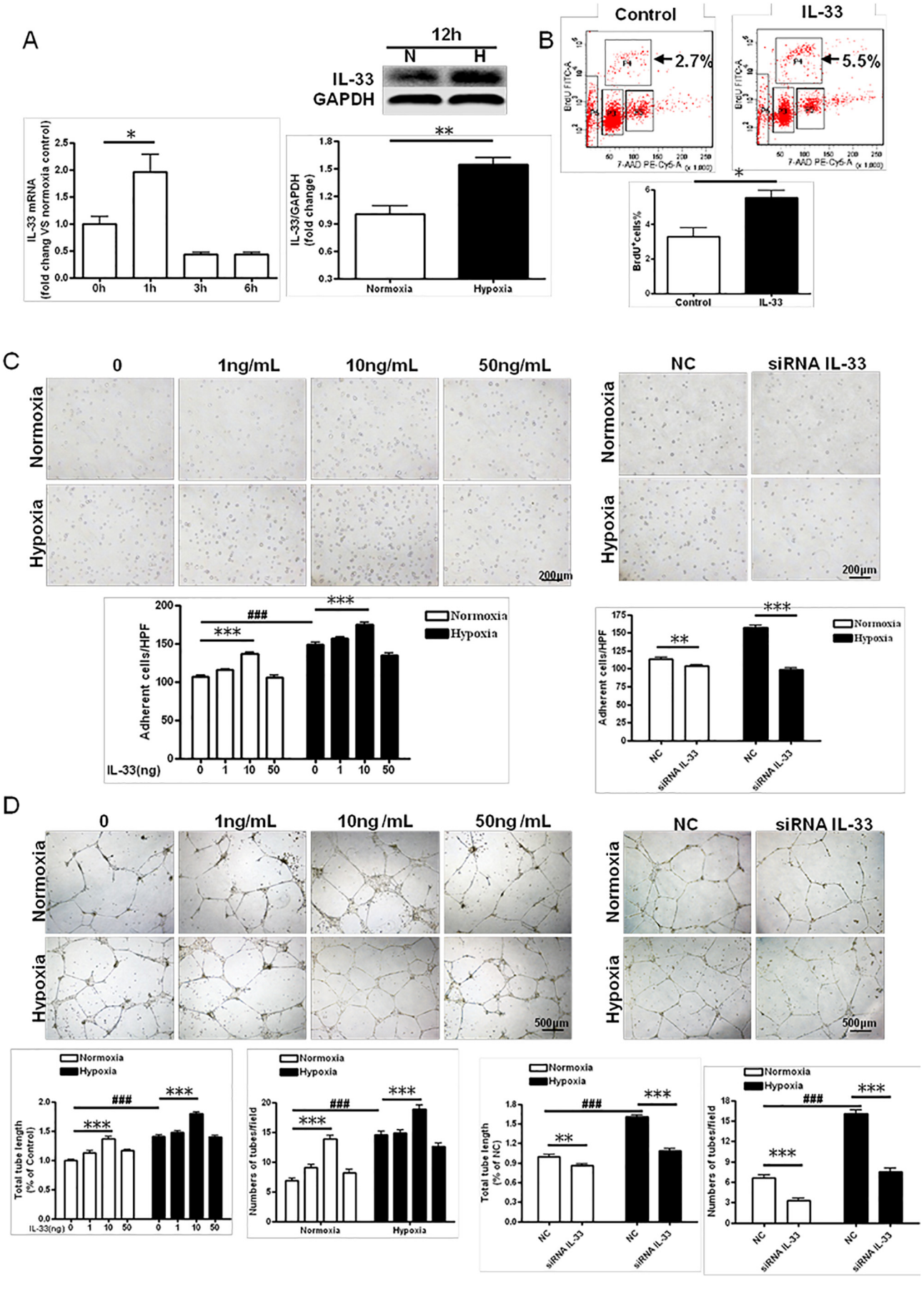
A
12h
N
H
IL-33
GAPDH
IL-33 mRNA (fold chang VS normoxia control)
0h
1h
3h
6h
IL-33/GAPDH (fold change)
Normoxia
Hypoxia
B
Control
IL-33
2.7%
5.5%
BrdU FITC-A
7-AAD PE-Cy5-A
BrdU+cells%
Control
IL-33
C
0
1ng/mL
10ng/mL
50ng/mL
Normoxia
Hypoxia
200μm
NC
siRNA IL-33
Adherent cells/HPF
IL-33(ng)
D
500μm
Total tube length (% of Control)
Numbers of tubes/field
Total tube length (% of NC)

8, Dojindo, Japan). Briefly, HPASMCs were seeded at 5×10^3cells per well in a 96-well plate, then incubated at 37 °C for 24 h before adding rhIL-33 (R&D Systems) at final concentrations of 10 ng/mL or normal saline control in a total volume of 200 μL in culture medium without foetal bovine serum (FBS). Cells were cultured with platelet-derived growth factor (rhPDGF, 10 ng/mL, R&D Systems) as a positive control. After incubation for a further 24 h, 10 μL of CCK-8 solution were added to each well and the cells incubated for a further 4 h. The absorbance of the medium at 450 nm was measured with Perkin Elmer EnSpire® Multimode Plate Reader (Waltham, MA, USA).

2.7. Endothelial Cell Adhesion and Tube Formation Assays

HPAECs were incubated with different concentrations of IL-33 or siRNAs specific for IL-33, ST2 or HIF-1α for 24 h. Cellular adhesion, tube formation, tube lengths and numbers were quantified using Image J and NIS-Elements BR Analysis (Nikon) [18].

2.8. Cell Co-culture Assay

To explore whether experimentally manipulated HPAECs affect the function of HPASMCs, we employed a non-contact, transwell co-culture model [19]. To measure cellular proliferation, 8×10^4 HPAECs per well were seeded into 12-well culture dishes, while HPASMCs at a density of 3×10^4 per insert were seeded into permeable (0.4 μm pore) transwell culture inserts (Millipore, MA, USA). HPASMCs were starved by culture in SMCM containing 2% FBS for 24 h, then the transwell inserts positioned into the wells of the HPAECs culture plates to establish co-culture conditions for a further 24 h in a mixed medium (1:1) mixture of ECM:SMCM (basic culture medium for endothelial cells and smooth muscle cells) with or without IL-33 (10 ng/mL). Following culture, the membranes of the inserts were washed with PBS twice, fixed in 4% paraformaldehyde for 30 min, then removed and the cellular nuclei stained with DAPI. The numbers of HPASMCs on the upper surfaces of the membranes were counted under high-power magnification using a microscope digital camera (Nikon, Japan). To measure cellular migration, HPAECs (1×10^5cells/well) were seeded into 12-well culture dishes, while arrested HPASMCs (1×10^5cells/per insert) were seeded into permeable (8 μm pore) transwell culture inserts which were then positioned into the wells of the HPAECs culture plates. After 24 h, the upper surfaces of the membrane inserts were washed with PBS twice and swabbed with a cotton bud to remove non-migrated cells. Migrated cells on the lower surface of the membrane were fixed in 4% paraformaldehyde for 30 min, then their nuclei stained with DAPI and counted as described above.

2.9. Cellular Transfection with Small Interfering RNA (siRNA) Species

HPAECs were transiently transfected with siRNA species in Opti-MEM medium (Invitrogen, Carlsbad, CA) using Lipofectamine RNAiMAX (Invitrogen, Carlsbad, CA) according to the manufacturer's instructions. The efficiency of siRNA transfection was measured by qRT-PCR or Western blot analysis. The sequences of siRNA used in the experiments were as follows:

(IL-33): sense: 5′-GCU CUG GCC UUA UGA UAA ATT-3′; and.
anti-sense: 5′-UUU AUC AUA AGG CCA GAG CTT-3′.
(ST2): sense: 5′-GCG AAU GUC ACC AUA UAU ATT-3′; and.
anti-sense: 5′-UAU AUA UGG UGA CAU UCG CTT-3′.
(HIF-1α): sense: 5′-GGC CGC UCA AUU UAU GAA UTT-3′; and.
anti-sense: 5′-AUU CAU AAA UUG AGC GGC CTT-3′.
(VEGFA): sense: 5′-GGC AGC UUG AGU UAA ACG ATT-3′; and.
anti-sense: 5′-UCG UUU AAC UCA AGC UGC CTT-3′.
(VEGFR-2): sense: 5′-CUC GGU CAU UUA UGU CUA UTT-3′; and.
anti-sense: 5′-AUA GAC AUA AAU GAC CGA GTT-3′.
Non-specific siRNA sequences were used as negative controls:
sense: 5′-UUC UCC GAA CGU GUC ACG UTT-3′; and.
anti-sense: 5′-ACG UGA CAC GUU CGG AGA ATT-3′.
(GenePharma, Shanghai, China).

2.10. qRT-PCR

Total RNA was extracted from lung tissue or cultured HPAECs using Trizol reagents (Sigma-Aldrich, USA). Reverse transcription was performed using the Superscript III First-strand Synthesis System (Invitrogen, USA) and quantitative, real-time PCR with Power SYBR Green PCR Master Mix (Applied Biosystems, UK) using a Mx3000P System (Stratagene, USA) as previously conducted in our laboratory.[36] The relative abundance of IL-33 and ST2 mRNA in HPAECs was normalised to that of GAPDH using a comparative cycle threshold method ($2^{-\Delta\Delta CT}$). The primer sequences were as listed below:

IL-33: sense: 5′-GGAGTGCTTTGCCTTTGGTA-3′;
anti-sense: 5′-CCATCAACACCGTCACCTG -3′.
ST2: sense: 5′-CAACTGGACAGCACCTCTTG-3′;
anti-sense: 5′-GGTGTAATCACCTGCGTCCT -3′.
GAPDH: sense: 5′-CGGAGTCAACGGATTTGGTCGTAT-3′;
anti-sense: 5′-AGCCTTCTCCATGGTGGTGAAGAC-3′.

2.11. Western Blotting

Equal amounts of protein extracted from lung tissue and HPAECs were separated by sodium dodecyl sulphate-polyacrylamide gel (SDS-PAGE) electrophoresis then transferred to a nitrocellulose membrane (NC, 0.45 μm, Millipore, USA). After blocking with 5% non-fat milk for 1 h at room temperature, the membrane was incubated with primary antibodies specific for IL-33 (mouse mAb, 1:200 dilution, Abcam), β-actin (rabbit mAb, 1:2000 dilution, Sigma-Aldrich), GAPDH (rabbit mAb, 1:2000 dilution, Sigma-Aldrich, USA), ST2 (rabbit mAb, 1:200 dilution, Abcam), HIF-1α (rabbit mAb, 1:50 dilution, Abcam), VEGFA (rabbit mAb, 1:100 dilution, Abcam), VEGFR-2 (rabbit mAb, 1:200 dilution, Cell Signalling Technology, USA) and ICAM (rat mAb, 1:200 dilution, Cell Signalling Technology) overnight at 4 °C. The membrane was then washed in PBST (0.1% Tween 20-PBS, Sigma-Aldrich) thrice for 10 min and incubated with IRDye800-conjugated secondary antibody (mouse or rabbit mAb, 1:10000, Odyssey LI-COR, USA) for 1 h. After washing in PBST thrice for 10 min again, the membrane staining was visualised using the LI-COR Odyssey imaging system. The protein signals were quantified using Image J and their relative expression normalised to that of GAPDH or β-actin as house-keeping protein or as ratios of their respective maximal expression.

2.12. Statistical Analysis

All data are expressed as the mean ± standard error of the mean (SEM) and were analyzed using GraphPad Prism 5.0 (GraphPad Software, USA). One-way analysis of variance (ANOVA) moderated by Tukey's Multiple Comparison correction was used to detect variation between 3 or more groups. Comparison between two groups was conducted using the two-tailed, unpaired Student's *t*-test. Statistical significance was defined as $P < 0.05$.

3. Results

3.1. Elevated Lung Tissue Expression of IL-33 and ST2 in A Murine Model of HPH and Human Subjects With Bronchiectasis Complicated by PH

The mean right ventricular systolic pressure (RVSP) and right ventricular hypertrophy index (RVHI), major feature of HPH, were substantially elevated in mice with PH induced by exposure to a hypoxic environment for 4 weeks (H4W) compared with control mice exposed to normal air (N4W) (Fig. 1 A, $p < 0.001$, respectively). Immunoreactivity for IL-33 and ST2 was elevated in the lung sections of mice with hypoxia-induced PH and localised principally to the airways epithelium

and pulmonary vascular endothelium (Fig. 1 B). Western blotting further confirmed that the IL-33 and ST2 protein expression was significantly increased in the murine lung tissue of the animals to hypoxia compared with normoxia (Fig. 1 C, $p < 0.05$).

Immunoreactivity for IL-33 and ST2 also significantly increased in lung sections from patients with bronchiectasis complicated by PH compared with normals, predominantly in the endothelial cells of the pulmonary arterioles (Fig. 2 A and B, IL-33: $p < 0.01$, ST2: $p < 0.05$).

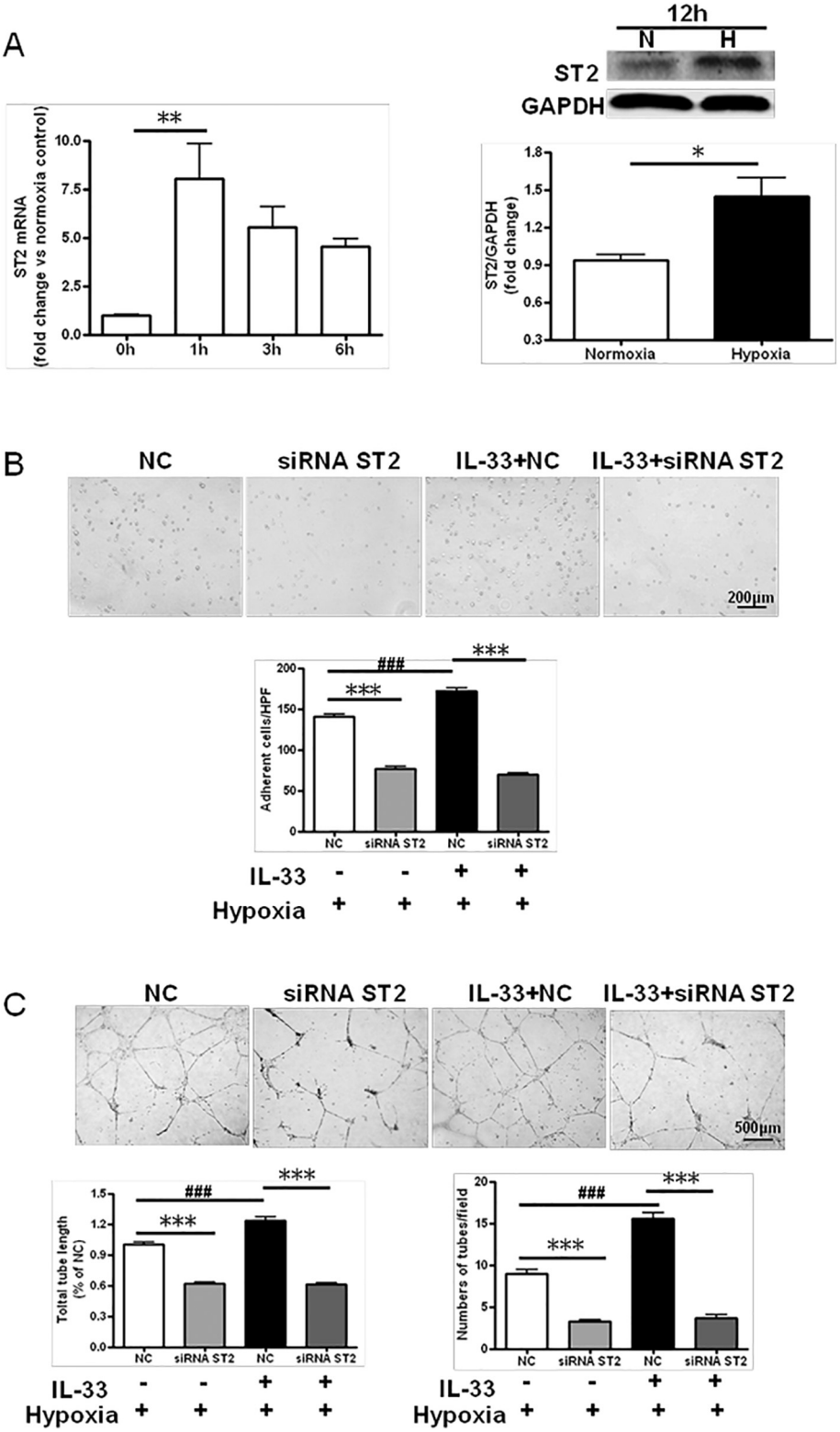

Fig. 6. IL-33 regulates the function of HPAECs *via* ST2. (A) Effects of hypoxia on expression of *St2* mRNA (left) and protein (right) by HPAECs ($n = 4$). $^{*}p < 0.05$, $^{**}p < 0.01$. (B) Effects of knock down of ST2 expression with siRNA on hypoxia- and IL-33-induced adhesion of HPAECs (mean ± SEM, $n = 5$). The results are expressed as numbers of cells per high power field. $^{***}p < 0.001$, $^{\#\#\#}p < 0.001$. (C) Effects of knock down of ST2 expression with siRNA on hypoxia- and IL-33-induced angiogenesis by HPAECs ($n = 6$). The results are expressed as the mean total tube lengths (percentages of medium control values) and numbers of tubes per field, respectively. $^{***}p < 0.001$, $^{\#\#\#}p < 0.001$.

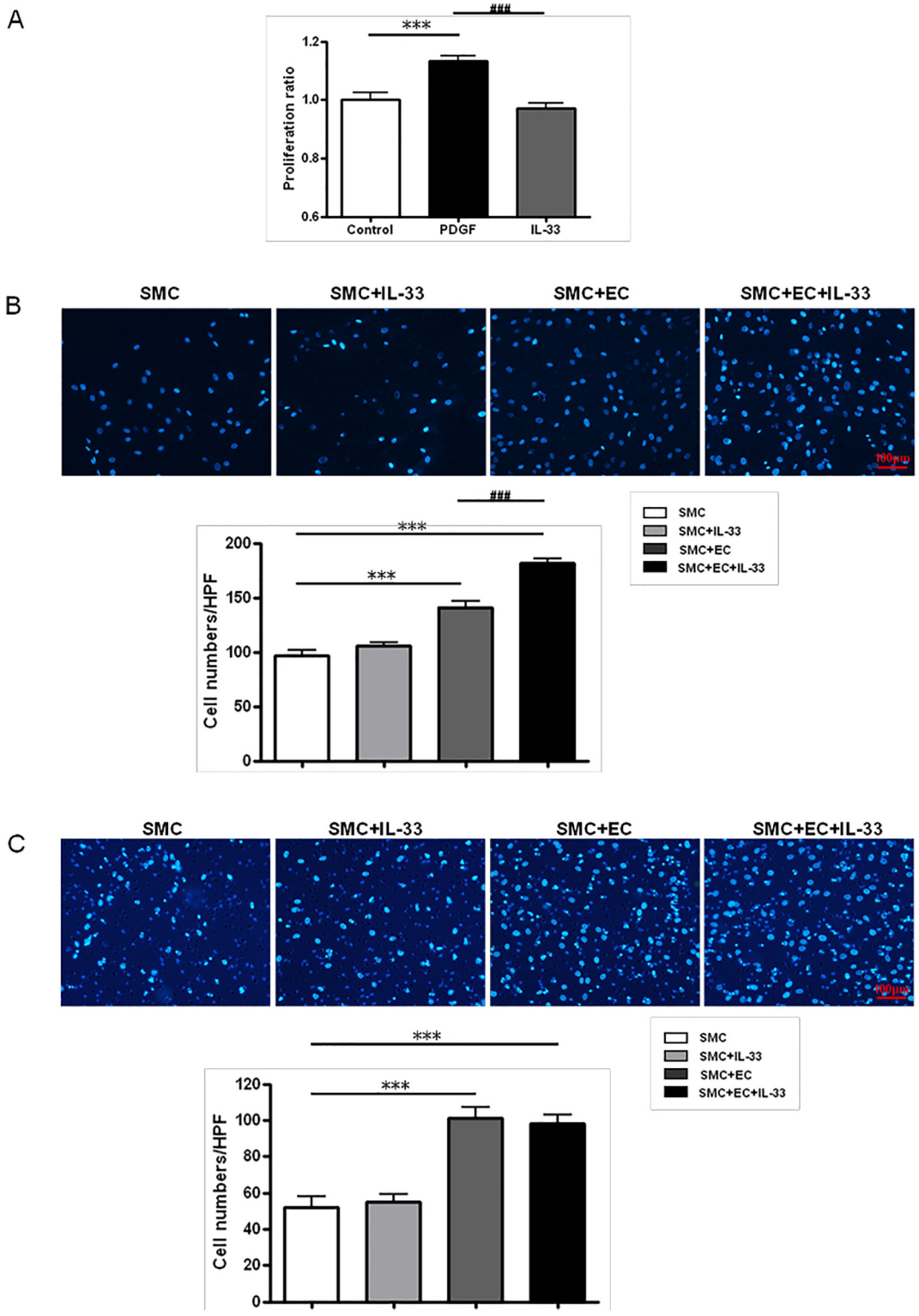

Fig. 7. Effects of co-culture with HPAECs on proliferation and migration of HPASMCs in the presence/absence of IL-33. (A) IL-33 alone did not affect proliferation of HPASMCs, while positive control PDGF promoted the proliferation of HPASMCs ($n = 6$ each group). $^{***}p < 0.001$, $^{\#\#\#}p < 0.001$. (B) The effect of IL-33 on proliferation of HPASMCs (labelled SMC) when co-cultured with HPAECs (labelled EC) ($n = 6$ each group). $^{***}p < 0.001$, $^{\#\#\#}p < 0.001$. (C) The effect of IL-33 on migration of HPASMCs (labelled SMC) when co-cultured with HPAECs (labelled EC) ($n = 6$ each group). $^{***}p < 0.001$.

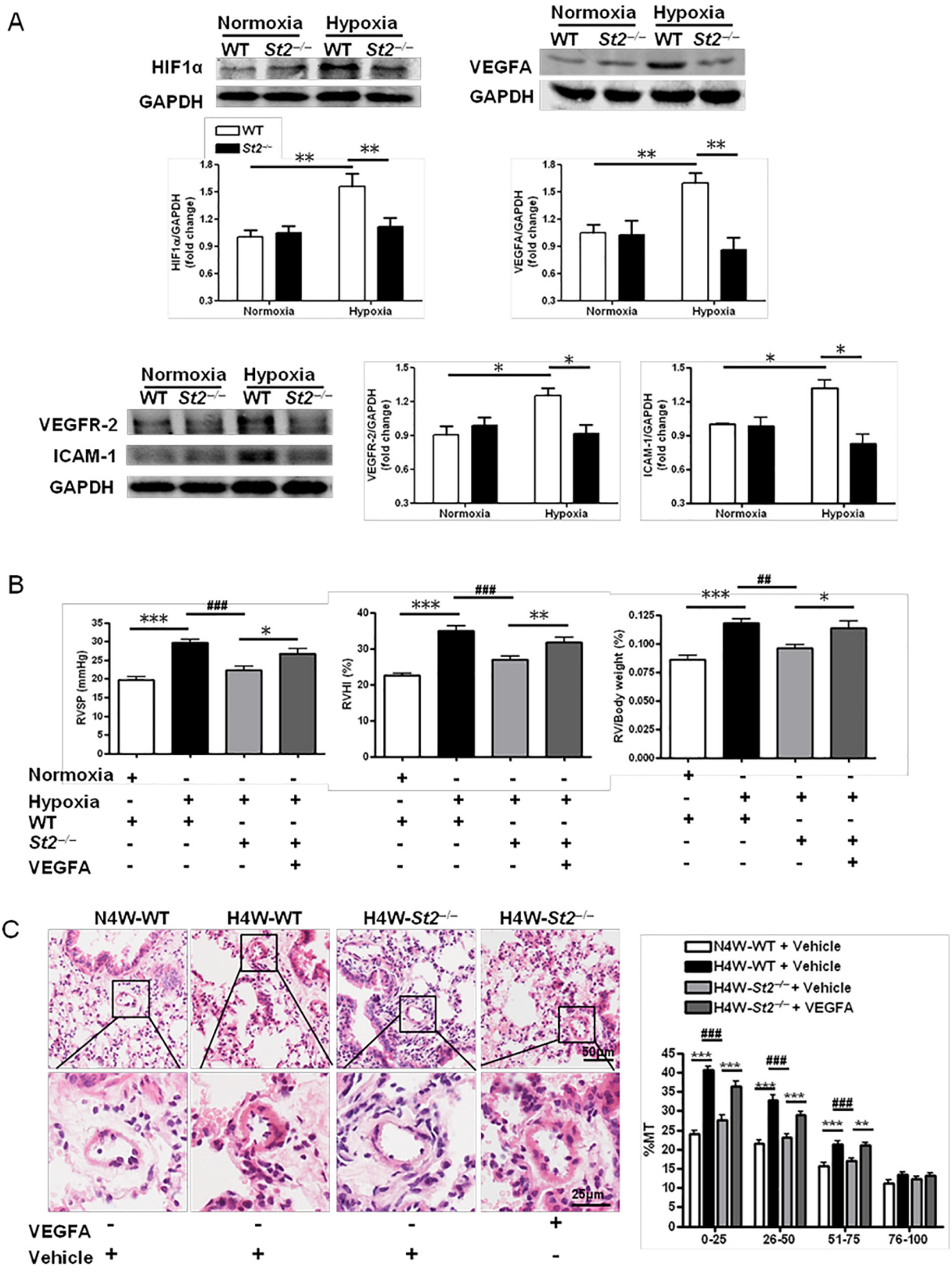

Fig. 8. Attenuated hypoxia-induced pulmonary vascular remodelling in $St2^{-/-}$ mice reflects reduced expression of HIF-1α/VEGFA/VEGFR-2. (A) Western blot analysis of HIF-1α, VEGFA, VEGFR-2 and ICAM-1 in lung tissues of WT and $St2^{-/-}$ mice following exposure to normoxia and hypoxia *in vivo* ($n = 3$–7). $^{*}p < 0.05$, $^{**}p < 0.01$. (B) RVSP, RVHI and RV/body weight ratios of WT mice exposed to normoxia and hypoxia, and $St2^{-/-}$ mice exposed to hypoxia with or without exogenous VEGFA ($n = 6$–8 each group). $^{*}p < 0.05$, $^{**}p < 0.01$, $^{***}p < 0.001$, $^{\#\#}p < 0.01$, $^{\#\#\#}p < 0.001$. (C) Pulmonary vascular remodelling in WT mice exposed to normoxia and hypoxia, and $St2^{-/-}$ mice exposed to hypoxia with or without exogenous VEGFA ($n = 4$ each group). (left) H&E staining of pulmonary arterioles. (right) Percentage medial thickness (%MT) of pulmonary arterioles grouped according to external diameter (μm). $^{**}p < 0.01$, $^{***}p < 0.001$, $^{\#\#\#}p < 0.001$.

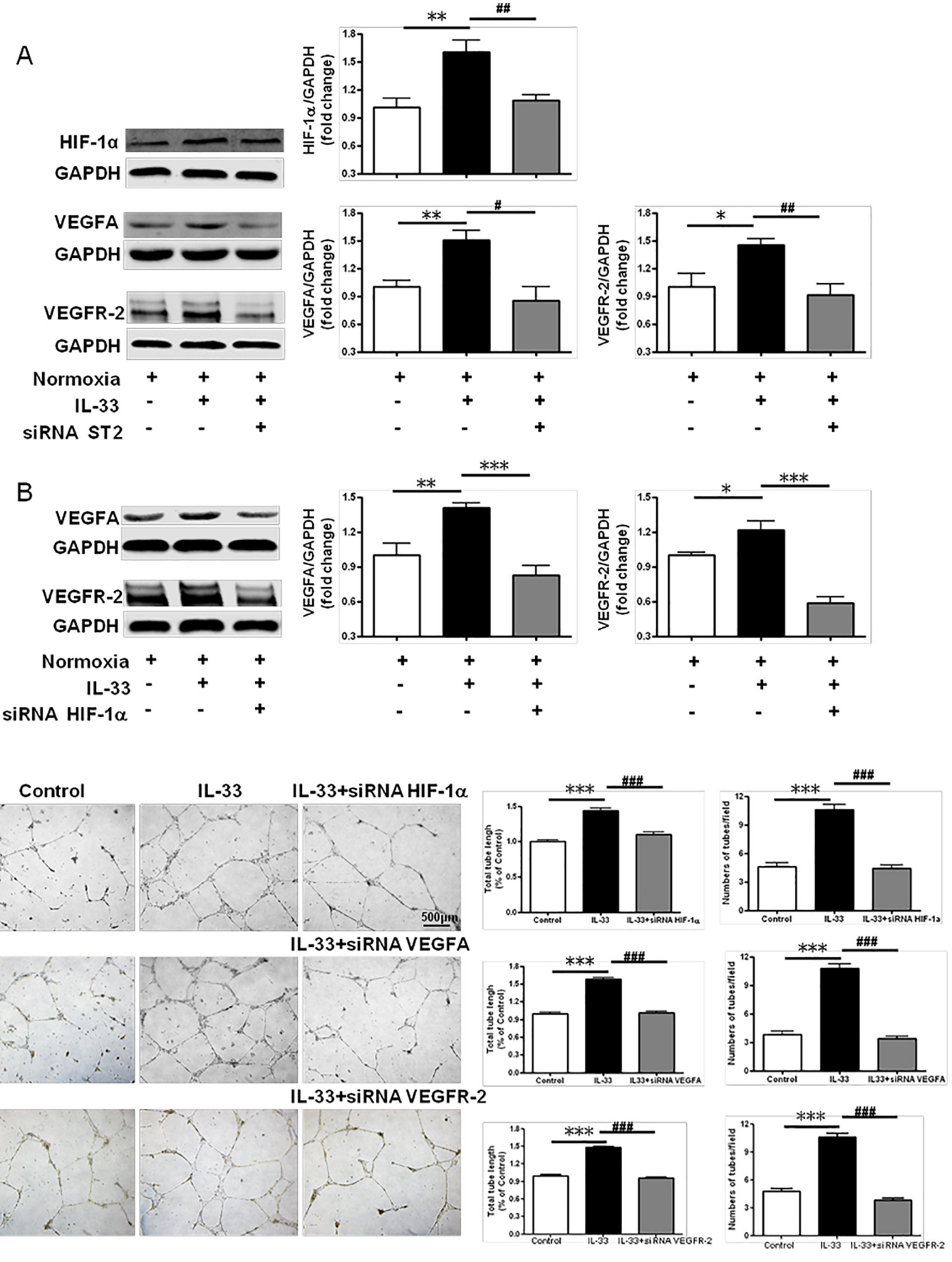
A
HIF-1α
GAPDH
VEGFA
GAPDH
VEGFR-2
GAPDH
Normoxia + + +
IL-33 - + +
siRNA ST2 - - +
HIF-1α/GAPDH (fold change)
VEGFA/GAPDH (fold change)
VEGFR-2/GAPDH (fold change)
B
VEGFA
GAPDH
VEGFR-2
GAPDH
Normoxia + + +
IL-33 - + +
siRNA HIF-1α - - +
C
Control
IL-33
IL-33+siRNA HIF-1α
500μm
IL-33+siRNA VEGFA
IL-33+siRNA VEGFR-2
Total tube length (% of Control)
Numbers of tubes/field
Control
IL-33
IL-33+siRNA HIF-1α
IL-33+siRNA VEGFA
IL-33+siRNA VEGFR-2

3.2. $St2^{-/-}$ Mice Show Attenuated, Hypoxia-induced Pulmonary Vascular Remodelling and Hypertrophy of Individual Cardiomyocytes of the RV and are Resistant to the Development of Hypoxia-induced PH

H&E staining (Fig. 3 A, top panel) and immunofluorescent staining of alpha-smooth muscle actin (α-SMA) (Fig. 3 A bottom panel) showed that the mean percentage medial thickness (%MT) of the arterioles was significantly elevated in WT mice following exposure to hypoxia, an effect which was significantly attenuated in the $St2^{-/-}$ mice, at least in vessels of diameter 75 μm or less (Fig. 3 A, right, $p < 0.001$).

H&E staining showed that hypoxia resulted in a significant elevation of the mean diameter of the cardiomyocytes in the right ventricle in the WT mice (Fig. 3 B, bottom panel, $p < 0.001$), consistent with the presence of hypoxia-triggered right ventricular hypertrophy, a hallmark of end-stage pulmonary hypertension [20], an effect almost completely abrogated in $St2^{-/-}$ mice ($p < 0.001$). No such changes were observed in the left ventricular cardiomyocytes in the WT or the $St2^{-/-}$ mice whether exposed to normoxia or hypoxia.

Haemodynamics analysis showed that hypoxia-exposed WT, but not $St2^{-/-}$ mice developed pulmonary hypertension characterised by significant elevation of the mean RVSP, RVHI and RV/body weight ratio in response to chronic hypoxia as compared with the control, normoxic group (Fig. 3 C, $p < 0.001$, respectively), although there were no significant changes in these indices in $St2^{-/-}$ and WT mice exposed to normoxia (Fig. 3 C). Correspondingly, hypoxia-exposed $St2^{-/-}$ mice developed a significantly lower mean RVSP, RVHI and RV/body weight ratio compared with the WT mice (Fig. 3 C $p < 0.001$, respectively).

3.3. Effects of Exogenous IL-33 on HPH

To clarify the effects of exogenous IL-33 on HPH, WT mice were exposed to normobaric hypoxia for 4 weeks concomitantly with intraperitoneal injections of IL-33 or normal saline (twice weekly, rmIL-33, 1 μg/dose/mouse). Compared with the saline control, IL-33 further aggravated pulmonary hypertension in mice exposed to hypoxia, as shown by significant elevation of the mean RVSP ($p < 0.001$) and RVHI ($p < 0.01$) (Fig. 3 D, left panel). In addition, H&E staining showed that IL-33 compared with saline treatment was associated with further, significant elevation of %MT of the pulmonary arterioles with external diameters <75 μm (Fig. 3 D, middle and right panels, $p < 0.01$ and $p < 0.001$, respectively).

3.4. Effects of Exogenous IL-33 or of Depletion of ST2 on RV Wall Thickness and the Peak Velocity of Blood Flow

Transthoracic echocardiography showed that exposure of mice to exogenous IL-33 further increased the right ventricular (RV) wall thickness (Fig. 4 A), while transthoracic echocardiography confirmed this and also revealed further reduction of the peak velocity of blood flow in the pulmonary artery (Fig. 4 B and C). The changes were attenuated in the $St2^{-/-}$ mice compared with the WT mice following exposure to hypoxia (Fig. 4 D and E).

3.5. Hypoxia Induces Expression of IL-33 by HPAECs, While IL-33 Enhances Proliferation, Adhesion and Remodelling of HPAECs In Vitro

Q-PCR analysis revealed a transient increase in IL-33 mRNA expression by cultured HPAECs as early as 1 h following exposure to hypoxia (Fig. 5 A, left, $p < 0.05$), while Western blotting analysis confirmed elevated IL-33 protein 12 h after exposure (Fig. 5 A right, $p < 0.01$).

Recombinant human IL-33 (rhIL-33) *in vitro* significantly enhanced progression of the HPAECs into the S phase of cellular division, as shown by flow cytometric analysis of the cells following BrdU incorporation (Fig. 5 B, $p < 0.05$), suggesting that IL-33 is able to increase the proliferation of these cells even under conditions of normoxia. Furthermore, under conditions of both normoxia and hypoxia, rhIL-33 significantly and concentration-dependently further enhanced HPAECs' adhesion (Fig. 5 C left panel, $p < 0.001$). Knockdown of the *Il33* gene in the cells by siRNA transfection significantly abrogated the capacity under conditions of both normoxia and hypoxia (Fig. 5 C right panel, $p < 0.01$, $p < 0.001$ respectively).

Finally, similar effects were observed on the ability of the HPAECs to assemble into tubular vessels. Compared with normoxic conditions, hypoxia *in vitro* increased the lengths and numbers of spontaneously formed tubules. Furthermore, rhIL-33 enhanced tubule formation in a concentration-dependent fashion (Fig. 5 D left panel, $p < 0.001$), while knockdown of the *Il33* gene almost completely attenuated the effects of hypoxia on this phenomenon (Fig. 5 D right panel, $p < 0.001$).

3.6. The ST2 Receptor Mediates the Effects of Hypoxia and Exogenous IL-33 Exposure on HPAECs

In order to clarify the role of IL-33 receptor ST2, we measured the expression of ST2 mRNA and protein by HPAECs. Q-PCR analysis showed that production of mRNA encoding ST2 was upregulated 8.05-fold at 1 h following exposure of the cells to hypoxia compared with normoxia (Fig. 6 A left, $p < 0.01$). Correspondingly, western blotting showed that ST2 protein was upregulated up to 1.55-fold at 12 h after hypoxia exposure (Fig. 6 A right, $p < 0.05$). Furthermore, knockdown of the *St2* gene not only attenuated their capacity to adhere and form tubules when exposed to hypoxia, but also abrogated the effects of exogenous IL-33 under conditions of both normoxia and hypoxia (Fig. 6 B and C, $p < 0.001$ in each case).

3.7. IL-33 Enhanced Proliferation of HPASMCs When Co-cultured With HPAECs

In our *in vitro* proliferation assay, co-culture of HPAECs with HPASMCs induced proliferation of the latter (Fig. 7 B, $p < 0.001$ compared with SMC monoculture), an effect which was further enhanced by rhIL-33 ($p < 0.001$), although IL-33 alone under these conditions did not significantly alter proliferation of the HPASMCs when cultured in isolation (Fig. 7 A). In addition, co-culture of HPAECs with HPASMCs also increased spontaneous HPASMC migration (Fig. 7 C $p < 0.001$), although this effect was not further enhanced by rhIL-33, while IL-33 alone did not induce HPASMC migration in the absence of HPAECs.

3.8. Attenuation of Hypoxia-induced Pulmonary Vascular Remodelling in $St2^{-/-}$ Mice Reflects Reduced Expression of HIF-1α/VEGFA/VEGFR-2

Compared with normoxia, hypoxia increased expression of HIF-1α protein in the lung tissue of the WT mice, but not in the $St2^{-/-}$ mice (Fig. 8 A, $p < 0.01$). In contrast, deletion of the *St2* gene did not influence HIF-1α expression in mice exposed to normoxia. Similarly, hypoxia also increased expression of VEGFA and VEGFR-2 protein in the lung tissues of the WT mice (Fig. 8 A, $p < 0.01$, $p < 0.05$ respectively), an effect again completely abrogated in the $St2^{-/-}$ mice (Fig. 8 A $p < 0.05$). Again,

Fig. 9. IL-33/ST2 enhances angiogenetic activity of HPAECs through the HIF-1α/VEGFA/VEGFR-2 axis. (A) Western blot analysis of HIF-1α, VEGFA and VEGFR-2 protein expression in HPAECs incubated with exogenous IL-33 (10 ng/mL) or medium control following transfection with siRNA encoding ST2 or control ($n = 4$–7). $^{*}p < 0.05$, $^{**}p < 0.01$, $^{\#}p < 0.05$, $^{\#\#}p < 0.01$. (B) Western blot analysis of VEGFA and VEGFR-2 protein expression in HPAECs treated with exogenous IL-33 following transfection with siRNA encoding HIF-1α or control ($n = 4$). $^{*}p < 0.05$, $^{**}p < 0.01$, $^{***}p < 0.001$. (C) Angiogenetic ability of HPAECs treated with exogenous IL-33 following transfection with siRNAs encoding HIF-1α, VEGFA or VEGFR-2 ($n = 6$). The results are expressed as the mean total tube lengths (percentages of control values) and numbers of tubes per field. $^{***}p < 0.001$, $^{\#\#\#}p < 0.001$.

deletion of the *St2* gene did not affect expression of these proteins in animals exposed to normoxia. Finally, hypoxia was associated with elevated expression of ICAM-1 protein in the WT mice (Fig. 8 A, $p < 0.05$), which was also significantly diminished in the $St2^{-/-}$ mice (Fig. 8 A, $p < 0.05$).

To further clarify the importance of VEGF as a downstream signalling protein for the IL33/ST2 axis in HPH, hypoxia-exposed $St2^{-/-}$ and WT mice were injected intraperitoneally with recombinant mouse VEGFA protein (rmVEGFA, R&D Systems, 100 ng/dose/mouse, twice weekly). Again, VEGFA partially reversed the reductions in mean RVSP, RVHI and RV/body weight ratio observed in the $St2^{-/-}$ compared with the WT mice following exposure to hypoxia (Fig. 8 B, $p < 0.05$ and $p < 0.01$, respectively). Accordingly, H&E staining showed attenuated arterial remodelling in the $St2^{-/-}$ mice compared with the WT mice following exposure to hypoxia (Fig. 8 C left panel), with reduction in the %MT of pulmonary arterioles smaller than 75 μm in diameter, administration of exogenous VEGFA partially but significantly reversed these changes (Fig. 8 C right panel, $p < 0.001$ and $p < 0.01$, respectively).

In vitro, Western blotting showed that rhIL-33 treatment significantly increased expression of HIF-1α, VEGFA and VEGFR-2 protein by HPAECs (Fig. 9 A). Prior knockdown of the *St2* gene using siRNA completely abrogated such effects of IL-33. Furthermore, prior knockdown of the *Hif1α* gene completely abrogated the ability of IL-33 to increase the expression of VEGFA and VEGFR-2 (Fig. 9 B). Finally, prior knockdown of the genes encoding HIF-1α, VEGFA or VEGFR-2 completely abrogated the IL-33-induced angiogenetic activity of these cells at 24 h in a normoxic environment (Fig. 9 C).

4. Discussion

Although IL-33 has now been implicated in the pathogenesis of many lung inflammatory and remodelling processes [21–23], its possible role in the pathogenesis of HPH *per se* remains unclear. Our observation that the expression of IL-33 and its receptor ST2 is up regulated in pulmonary arterial endothelial cells in sections of lung tissue obtained from murine model of HPH and from patients with HPH impelled us further to explore the potential roles of IL-33/ST2/HIF-1α/VEGF signalling pathways in the pathogenesis of this phenomenon using *in vivo* and *in vitro* experiments.

Our data clearly support the hypothesis that exposure of the airways to hypoxia upregulates expression of IL-33/ST2 by lung structural cells, in particular pulmonary arterial endothelial cells, which in turn contributes to hypoxic pulmonary vascular remodelling at least partly through activating downstream of the IL-33/ST2 axis, in particular HIF-1α/VEGF signalling. Although it is well known that HIF-1α and VEGF are critical mediators in the phenomenon of hypoxia-induced vascular remodelling, so far as we are aware no study to date has addressed in detail the events upstream of these molecules, and in particular whether or not these upstream events are influenced by IL-33/ST2 signalling. In the present study, while knockdown of the gene encoding IL-33 receptor, ST2, did not alter the baseline expression of HIF-1α, VEGF and VEGFR-2 in the lung tissue of the experimental mice in normoxic conditions, it did reduce the elevated expression of all three proteins in response to hypoxia, suggesting that elevated production of IL-33, acting on its receptor ST2, in the presence of sustained hypoxia is a trigger for elevated production of HIF-1α and VEGF and the initiation of the vascular remodelling which results in HPH. This conclusion is further supported by our *in vitro* experiments in which knockdown of the ST2 gene in HPAECs abrogated the effects of exogenous IL-33 and/or hypoxia in upregulating the expression of HIF-1α, VEGFA and VEGFR-2. Additionally, exposure to IL-33 increased the proliferation, adhesiveness and angiogenetic activity of HPAECs, an effect abrogated by knockdown of any one of these mediators, suggesting that the end effect of activation of the IL-33/HIF-1α/VEGFA axis in these cells is to initiate and sustain the vascular remodelling which eventually results in HPH. This axis might also induce the right ventricular cardiomyocyte hypertrophy and pulmonary vascular hypertension associated with chronic hypoxia. Finally, the data suggest a role for this axis in further facilitating HPH by increasing the expression of cellular adhesion molecules (CAMs, in this case ICAM-1) which might promote inflammatory cellular infiltration and further facilitate remodelling.

We did not test however directly investigate whether blockade of endogenous IL-33 signalling (though blockade either of IL-33 production or blockade of ST2) reduces the hypoxia-induced proliferation of these cells in the present study. However, we did find that know down of IL-33 gene using the siRNA technique attenuated hypoxia-induced adhesion and tube formation by the HPAEC. We believe that it is reasonable to speculate that blockade of IL-33/ST2 signalling in HPAEC might exert a similar effect on proliferation of these cells because this is presumably a feature of the hypoxia-induced, structural reorganisation of these cells required for example for the formation of tubules. This would be an interesting focus for our continuing experiments in the future.

Not all existing studies in the literature suggest a detrimental role for IL-33 in mediating haemodynamic changes. For instance, in a murine model, administration of exogenous IL-33 was reported to reduce aortic atherosclerotic plaque formation and improve left ventricular function [24]. In contrast, it has been shown that IL-33 induced expression of tissue factor (TF) by human umbilical vein and coronary artery endothelial cells, suggesting that may induce thrombosis around atherosclerotic plaques in humans [25]. In addition, it has been shown that myocardial pressure overload from hypertension can induce IL-33 production by cardiovascular endothelial cells [26], which may induce local or even systemic inflammation. Here, exposure of WT mice to hypoxia induced obvious right, but not left ventricular hypertrophy as verified by alterations in single cardiomyocyte diameter, while knockdown of *St2* significantly abrogated this phenomenon, clearly implicating the IL-33/ST2 axis in the pathogenesis of HPH and consequent right heart failure. There are already several studies in the literature implicating HIF-1α and VEGF in the pathogenesis of the vascular remodelling which results in HPH [1, 2]. Increased expression of HIF-1α has been noted in the serum of patients with HPH and in the lungs in animal models [10]. Deletion of the HIF-1α gene has previously been reported to down-regulate VEGF signalling and abrogate haemodynamic changes in a murine model of HPH [11]. Ours is however the first study, to our knowledge, implicating a mechanistic interaction between IL-33, HIF-1α and VEGF in the pathogenesis of HPH.

It is known that structural cells of blood vessels such as smooth muscle cells and fibroblasts as well as endothelial cells can express IL-33 [6, 21]. Demyanets *et al.* observed that the large vessels and cardiac microvascular endothelial cells were the major sources expressing IL-33 and ST2 [27], suggesting that, *in vitro*, exogenous human IL-33 acts on vascular endothelial cells, but not cardiomyocytes, fibroblasts or vascular smooth muscle cells, at least in terms of eliciting production of other proinflammatory cytokines. A very recent study has reported that administration of IL-33 over a prolonged period results in the development of pulmonary arterial hypertrophy [28]. Our data showed that co-culture of vascular endothelial cells with smooth muscle cells significantly enhanced proliferation of the latter, an effect further enhanced in the presence of additional IL-33, while IL-33 alone exerted no such effect. This suggests that additional, IL-33-enhanced mediators derived from vascular endothelial cells may regulate smooth muscle proliferation. It is also well known that many other cell types may express the IL-33 receptor ST2, including inflammatory cells such as monocytes, raising the possibility that products of other adjacent structural cells activated through IL-33/ST2 may contribute to this phenomenon.

To conclude, our experiments show that IL-33 and its receptor ST2 are constitutively expressed by human pulmonary arterial endothelial cells and that hypoxia up regulates this expression. IL-33 acts on these cells to enhance proliferation, adhesion and angiogenesis in an ST2-dependent fashion. These effects of IL-33/ST2, operating through

activation of the HIF-1α/VEGF axis or otherwise, on pulmonary artery vascular endothelial cells may provide a basis for the initiation of vascular smooth muscle cell, and possibly also cardiomyocyte remodelling which eventually results in pulmonary hypertension, while hypoxia is one potential initiator for up regulation of the IL-33/ST2 axis.

Author Contributions

Kewu Huang, Sun Ying and Wei Wang designed research; Jie Liu, Wang Wang, Lei Wang and Shihao Chen undertook the research; Kewu Huang and Bo Tian contributed clinical samples; Jie Liu, Chris J. Corrigan, Sun Ying and Wei Wang analyzed data; Jie Liu, Chris J. Corrigan, Sun Ying and Wei Wang wrote the paper; and Chen Wang supported the research.

Conflict of Interest

The authors declare no conflict of interest.

Acknowledgements

The authors thank Prof. Ai-juan Qu and Dr. Wei Zhang of Capital Medical University for their assistance and guidance with identifying subjects and technical support with this work. The authors are also very grateful for Professor Andrew N.J. McKenzie of the Medical Research Council Laboratory of Molecular Biology, Cambridge, United Kingdom for his kind gift of the $St2^{-/-}$ mice.

Sources of Funding

This study was supported by the National Natural Science Foundation of China (81370152, 81471594, 81770049) and Beijing Municipal Natural Science Foundation (7142027).

References

[1] Pugliese SC, Poth JM, Fini MA, Olschewski A, El Kasmi KC, Stenmark KR. The role of inflammation in hypoxic pulmonary hypertension: from cellular mechanisms to clinical phenotypes. Am J Physiol Lung Cell Mol Physiol 2015;308(3):L229–52.
[2] Maron BA, Machado RF, Shimoda L. Pulmonary vascular and ventricular dysfunction in the susceptible patient (2015 Grover conference series). Pulm Circ 2016;6(4):426–38.
[3] Thompson AAR, Lawrie A. Targeting vascular remodeling to treat pulmonary arterial hypertension. Trends Mol Med 2017;23(1):31–45.
[4] Mohsenin V. The emerging role of microRNAs in hypoxia-induced pulmonary hypertension. Sleep Breath 2016;20(3):1059–67.
[5] Molofsky AB, Savage AK, Locksley RM. Interleukin-33 in tissue homeostasis, injury, and inflammation. Immunity 2015;42(6):1005–19.
[6] Byers DE, Alexander-Brett J, Patel AC, et al. Long-term IL-33-producing epithelial progenitor cells in chronic obstructive lung disease. J Clin Invest 2013;123(9):3967–82.
[7] Li D, Guabiraba R, Besnard AG, et al. IL-33 promotes ST2-dependent lung fibrosis by the induction of alternatively activated macrophages and innate lymphoid cells in mice. J Allergy Clin Immunol 2014;134(6):1422–32 [e11].
[8] Shan S, Li Y, Wang J, et al. Nasal administration of interleukin-33 induces airways angiogenesis and expression of multiple angiogenic factors in a murine asthma surrogate. Immunology 2016;148(1):83–91.
[9] An G, Zhang X, Wang W, et al. The effects of interleukin-33 on airways collagen deposition and matrix metalloproteinase expression in a murine surrogate of asthma. Immunology 2018. https://doi.org/10.1111/imm.12911.
[10] Jiang Y, Wang J, Tian H, et al. Increased SUMO-1 expression in response to hypoxia: interaction with HIF-1alpha in hypoxic pulmonary hypertension. Int J Mol Med 2015;36(1):271–81.
[11] Johns RA, Takimoto E, Meuchel LW, et al. Hypoxia-inducible factor 1alpha is a critical downstream mediator for hypoxia-induced Mitogenic factor (FIZZ1/RELMalpha)-induced pulmonary hypertension. Arterioscler Thromb Vasc Biol 2016;36(1):134–44.
[12] Sun M, He C, Wu W, et al. Hypoxia inducible factor-1alpha-induced interleukin-33 expression in intestinal epithelia contributes to mucosal homeostasis in inflammatory bowel disease. Clin Exp Immunol 2017;187(3):428–40.
[13] Theoharides TC, Zhang B, Kempuraj D, et al. IL-33 augments substance P-induced VEGF secretion from human mast cells and is increased in psoriatic skin. Proc Natl Acad Sci U S A 2010;107(9):4448–53.
[14] Balato A, Lembo S, Mattii M, et al. IL-33 is secreted by psoriatic keratinocytes and induces pro-inflammatory cytokines via keratinocyte and mast cell activation. Exp Dermatol 2012;21(11):892–4.
[15] Townsend MJ, Fallon PG, Matthews DJ, Jolin HE, Mckenzie AN. T1/ST2-deficient mice demonstrate the importance of T1/ST2 in developing primary T helper cell type 2 responses. J Exp Med 2000;191(6):1069–76.
[16] Wang W, Liu J, Ma A, et al. mTORC1 is involved in hypoxia-induced pulmonary hypertension through the activation of Notch3. J Cell Physiol 2014;229(12):2117–25.
[17] Jin Y, Wang W, Chai S, Liu J, Yang T, Wang J. Wnt5a attenuates hypoxia-induced pulmonary arteriolar remodeling and right ventricular hypertrophy in mice. Exp Biol Med (Maywood) 2015;240(12):1742–51.
[18] Xu T, Zhang Z, Liu T, et al. Salusin-beta contributes to vascular inflammation associated with pulmonary arterial hypertension in rats. J Thorac Cardiovasc Surg 2016;152(4):1177–87.
[19] Hergenreider E, Heydt S, Treguer K, et al. Atheroprotective communication between endothelial cells and smooth muscle cells through miRNAs. Nat Cell Biol 2012;14(3):249–56.
[20] Sun X, Ku DD. Rosuvastatin provides pleiotropic protection against pulmonary hypertension, right ventricular hypertrophy, and coronary endothelial dysfunction in rats. Am J Physiol Heart Circ Physiol 2008;294(2):H801–9.
[21] Liew FY, Girard JP, Turnquist HR. Interleukin-33 in health and disease. Nat Rev Immunol 2016;16(11):676–89.
[22] Bertheloot D, Latz E. HMGB1, IL-1alpha, IL-33 and S100 proteins: dual-function alarmins. Cell Mol Immunol 2017;14(1):43–64.
[23] Zhao J, Zhao Y. Interleukin-33 and its receptor in pulmonary inflammatory diseases. Crit Rev Immunol 2015;35(6):451–61.
[24] Griesenauer B, Paczesny S. The ST2/IL-33 Axis in immune cells during inflammatory diseases. Front Immunol 2017;8:475.
[25] Stojkovic S, Kaun C, Basilio J, et al. Tissue factor is induced by interleukin-33 in human endothelial cells: a new link between coagulation and inflammation. Sci Rep 2016;6:25171.
[26] Chen WY, Hong J, Gannon J, Kakkar R, Lee RT. Myocardial pressure overload induces systemic inflammation through endothelial cell IL-33. Proc Natl Acad Sci U S A 2015;112(23):7249–54.
[27] Demyanets S, Kaun C, Pentz R, et al. Components of the interleukin-33/ST2 system are differentially expressed and regulated in human cardiac cells and in cells of the cardiac vasculature. J Mol Cell Cardiol 2013;60:16–26.
[28] Ikutani M, Tsuneyama K, Kawaguchi M, et al. Prolonged activation of IL-5-producing ILC2 causes pulmonary arterial hypertrophy. JCI Insight 2017;2(7):e90721.